Immunization with a functional protein complex required for erythrocyte invasion protects against lethal malaria

Prakash Srinivasan[a,1], Emmanuel Ekanem[b], Ababacar Diouf[a], Michelle L. Tonkin[c], Kazutoyo Miura[a], Martin J. Boulanger[c], Carole A. Long[a], David L. Narum[b], and Louis H. Miller[a,1]

[a]Laboratory of Malaria and Vector Research and [b]Laboratory of Malaria Immunology and Vaccinology, National Institutes of Allergy and Infectious Diseases, National Institutes of Health, Rockville, MD 20852; and [c]Department of Biochemistry and Microbiology, University of Victoria, Victoria, BC, Canada V8W 3P6

Contributed by Louis H. Miller, June 2, 2014 (sent for review April 24, 2014; reviewed by Robert Sauerwein and Christopher Plowe)

An essential step in the invasion of red blood cells (RBCs) by *Plasmodium falciparum* (*Pf*) merozoites is the binding of rhoptry neck protein 2 (RON2) to the hydrophobic groove of apical membrane antigen 1 (AMA1), triggering junction formation between the apical end of the merozoite and the RBC surface to initiate invasion. Vaccination with AMA1 provided protection against homologous parasites in one of two phase 2 clinical trials; however, despite its ability to induce high-titer invasion-blocking antibodies in a controlled human challenge trial, the vaccine conferred little protection even against the homologous parasite. Here we provide evidence that immunization with an AMA1-RON2 peptide complex, but not with AMA1 alone, provided complete protection against a lethal *Plasmodium yoelii* challenge in mice. Significantly, IgG from mice immunized with the complex transferred protection. Furthermore, IgG from *Pf*AMA1-RON2–immunized animals showed enhanced invasion inhibition compared with IgG elicited by AMA1 alone. Interestingly, this qualitative increase in inhibitory activity appears to be related, at least in part, to a switch in the proportion of IgG specific for certain loop regions in AMA1 surrounding the binding site of RON2. Antibodies induced by the complex were not sufficient to block the FVO strain heterologous parasite, however, reinforcing the need to include multiallele AMA1 to cover polymorphisms. Our results suggest that AMA1 subunit vaccines may be highly effective when presented to the immune system as an invasion complex with RON2.

Malaria caused by *Plasmodium falciparum* (*Pf*) remains one of the leading causes of mortality in pregnant women and children in sub-Saharan Africa (1). The lack of a vaccine and resistance to front-line antimalarials pose a global public health threat. RTS,S, a leading vaccine candidate that targets the initial infection of the liver, has demonstrated only partial efficacy (2). Clinical manifestations of malaria are caused by the blood-stage parasites that reside within red blood cells (RBCs); thus, vaccines targeting the erythrocytic forms of the parasite are desirable for efficient disease control.

Apical membrane antigen 1 (AMA1) was once considered a leading blood-stage vaccine candidate, because antibodies against recombinant AMA1 are highly efficient in blocking entry of parasites into RBCs both in vitro and in immunized nonhuman primates in vivo (3, 4). Disappointingly, however, despite these early successes, moderate to no efficacy was observed in human trials (5–7). Previous in vitro assays have shown that AMA1 polymorphisms among different parasite strains rendered the antibodies allele-specific (8, 9); however, the failure in a controlled human clinical trial cannot be attributed to polymorphisms, given that the vaccine was not efficient even against homologous parasites (5). Although the vaccinations failed to induce immunity against the homologous parasite in vivo, AMA1-specific antibodies purified from these individuals blocked parasite invasion in vitro (5).

Two phase 2 trials have been reported to date (6, 7). Ouattara et al. (6) reported no significant efficacy of a bivalent AMA1 vaccine adjuvanted with aluminum hydroxide even against homologous parasites, whereas Thera et al (7), in a study of a monovalent AMA1 vaccine with a different adjuvant system, found 64% efficacy against vaccine-type allele as defined by amino acid homology in the domain Id loop (cluster 1L). The number of vaccine-type parasites in that study population was very low (~5%), however, and whether this level of efficacy can be achieved in a larger sample size remains to be determined. That study also confirmed the importance of polymorphisms in AMA1 contributing to lack of efficacy against heterologous parasites (7, 10). Recent efforts to cover the polymorphism in AMA1 demonstrated that combining four or five different AMA1 alleles could overcome the strain-specific barrier in vitro (9, 11, 12). Nonetheless, the discordance between failure to protect humans in vivo and ability to block vaccine-type parasite invasion in vitro (5) underscores the need to improve AMA1 vaccine efficacy against homologous parasites.

It was recently reported that AMA1 interacts with a conserved 49-aa region of RON2, a parasite rhoptry-resident protein, during merozoite invasion (13–15). Small molecules or peptides that block this interaction inhibit merozoite invasion (16, 17), highlighting the important role of this protein–protein

Significance

Apical membrane antigen 1 (AMA1) is a leading blood-stage vaccine candidate. Despite the vaccine's ability to elicit high-titer AMA1-specific antibodies, it showed little efficacy in clinical trials against a homologous parasite. AMA1 interacts with a 49-aa region of rhoptry neck protein 2 (RON2), another parasite protein, during merozoite invasion. In this study, we demonstrate that immunization with a functional complex of AMA1-RON2 peptide (RON2L) induces antibody-mediated complete protection against lethal *Plasmodium yoelli* challenge. Interestingly, the qualitative increase in efficacy appears to be related in part to a switch in the proportion of antibodies targeting the RON2-binding site in AMA1. Our data suggest that a multiallele AMA1 (to overcome polymorphisms) in complex with RON2L should be effective in protecting against all *Plasmodium falciparum* parasites.

Author contributions: P.S. and L.H.M. designed research; P.S., E.E., and A.D. performed research; P.S., E.E., M.L.T., and D.L.N. contributed new reagents/analytic tools; P.S., K.M., M.J.B., C.A.L., D.L.N., and L.H.M. analyzed data; and P.S., M.L.T., D.L.N., and L.H.M. wrote the paper.

Reviewers: R.S., Radboud University Nijmegen Medical Center; and C.P., Howard Hughes Medical Institute.

The authors declare no conflict of interest.

Freely available online through the PNAS open access option.

[1]To whom correspondence may be addressed. E-mail: srinivasanp@niaid.nih.gov or lmiller@niaid.nih.gov.

This article contains supporting information online at www.pnas.org/lookup/suppl/doi:10.1073/pnas.1409928111/-/DCSupplemental.

interaction. Analysis of the crystal structure of the complex revealed that the RON2 peptide (RON2L) binds to a conserved hydrophobic groove in AMA1, resulting in extensive conformational changes in certain loop regions surrounding the groove (18, 19). Antibodies that bind in or near the hydrophobic groove block parasite invasion by inhibiting the binding of RON2 (11, 15).

In this study, we evaluated a novel approach to enhancing the efficacy of the AMA1 vaccine using a highly virulent *Plasmodium yoelli* YM (*Py*YM) mouse model. Strikingly, all animals immunized with the AMA1-RON2L complex, but not those immunized with the individual antigens, were found to be protected against the virulent homologous *Py*YM challenge. Antibodies largely mediate this protection, as demonstrated by the fact that passive transfer of IgG, but not of T cells, from AMA1-RON2L–vaccinated animals controlled parasitemia. Furthermore, we found that the human parasite *Pf*3D7-AMA1-RON2L complex induced qualitatively higher growth inhibitory antibodies than AMA1 alone in in vitro assays. Surprisingly, our results indicate that the increase in inhibitory antibodies generated by the complex may be related in part to a switch in the proportion of antibodies against the loops surrounding the hydrophobic groove with which RON2 interacts. Our data suggest that a vaccine comprising a multiallele AMA1 in complex with RON2L may be more efficacious than AMA1 alone in targeting both homologous and heterologous parasites.

Results and Discussion

AMA1-RON2L Complex, but Not AMA1 Alone, Protects Against Lethal *Py*YM Challenge. We first tested whether AMA1 or RON2L can protect against a lethal *Py*YM parasite challenge. Animals were immunized with recombinant *Py*AMA1 or RON2L peptide conjugated to keyhole limpet hemocyanin (KLH) and challenged i.v. with *Py*YM-infected RBCs (iRBCs). All animals succumbed to the infection similar to control animals (Fig. 1*A*). This lack of protection against a homologous parasite challenge in animals vaccinated with AMA1 resembles the results from controlled human trials using *Pf* (5). Strikingly however, all animals immunized with the complex were protected against the lethal parasite challenge (Fig. 1 *A* and *B*). The amounts of anti-AMA1 antibodies were similar in the group immunized with the complex and the group immunized with AMA1 alone (Fig. 1*C*), suggesting that the differences observed between the groups were related to qualitative differences in antibody specificity.

If immunity to virulent infection were related to vaccination with a functional AMA1-RON2L complex, we would expect that mutating the cysteine residues in RON2L, which prevent complex formation with AMA1 (15) (Fig. 1 *D* and *E*), would fail to protect mice. Consistent with this idea, immunization with a mixture of AMA1-RON2L$_{c/a}$ failed to protect mice against *Py*YM (Fig. 1*F* and Fig. S1*A*).

To determine whether protection is related simply to an additive effect of immunizing with two antigens or whether a complex is required, we immunized animals with the AMA1-RON2L complex or with the two antigens, AMA1 and RON2L (AMA1+RON2L), injected in two separate sites (Fig. 1*G*). Whereas mice immunized with the AMA1-RON2L complex were protected, those immunized with the two antigens separately were not protected against *Py*YM (Fig. 1*G* and Fig. S1*B*). Our data indicate that protection against lethal *Py*YM parasites requires vaccination with a preformed AMA1-RON2L complex.

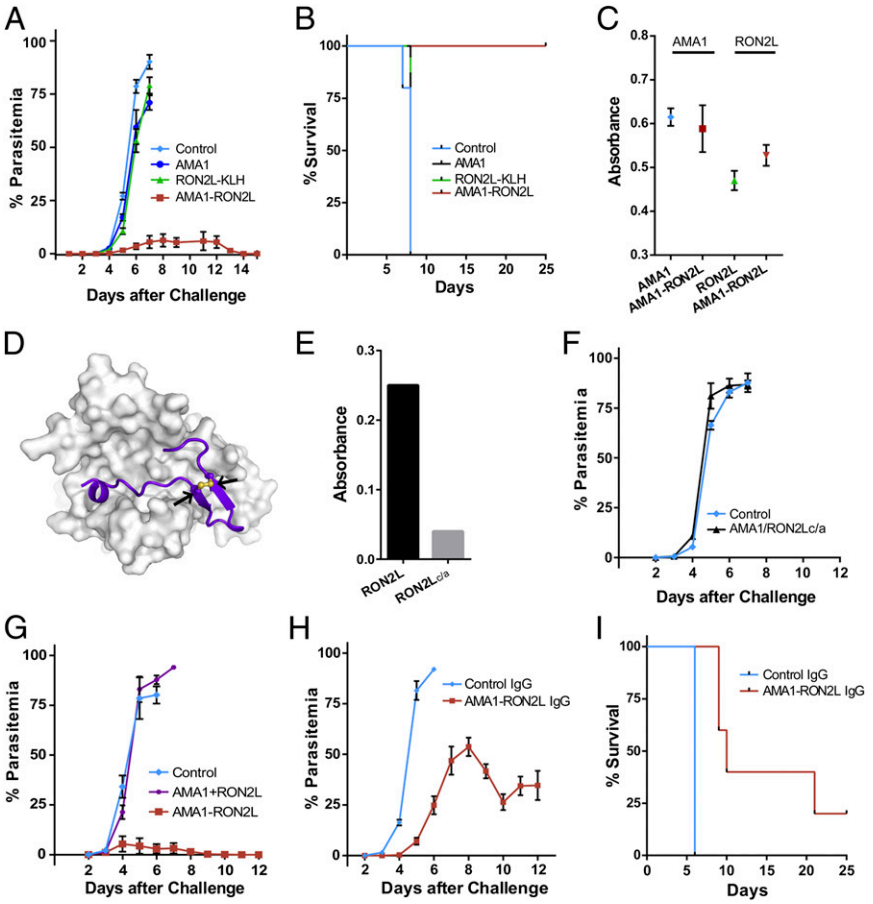

Fig. 1. Immunization with AMA1-RON2L complex but not AMA1 alone protects mice against lethal *Py*YM challenge. (*A*) Five mice per group were immunized with AMA1, RON2L-KLH, or AMA1-RON2L complex and then challenged with 10^4 iRBCs i.v. Five mice immunized with buffer in Freund's adjuvant were used as controls. Error bars indicate mean ± SEM. (*B*) Kaplan-Meir curve of the overall survival of animals in *A*. (*C*) ELISA titers of antibody response against AMA1 and RON2L from sera of mice from *A*. Sera were used at 1:8,000 and 1:2,000 dilutions for AMA1 and RON2L, respectively. Error bars indicate mean ± SEM at OD_{405}. (*D*) In silico homology model of *Py*AMA1-*Py*RON2L complex based on *Pf*AMA1-*Pf*RON2 complex structure. Arrows indicate the two cysteines in the *Py*RON2L peptide. (*E*) Mutation of Cys1856 and 1868 to Ala abolishes RON2L binding to *Py*AMA1. (*F*) Mutating the two cysteines to alanines (*c*/a) in the RON2L peptide required for binding to AMA1 abrogates complex-driven protection in mice. Five mice per group were challenged with 10^5 iRBCs. Error bars indicate mean ± SEM. (*G*) Protection requires vaccination with the AMA1-RON2L complex, because immunizing animals with the two antigens in separate sites (AMA1 + RON2L) does not confer protection. Five mice per group for the control and AMA1-RON2L groups and four mice for the AMA1+RON2L group were challenged with 10^5 iRBCs. Error bars indicate mean ± SEM. (*H*) Passive transfer of IgG from mice immunized with the AMA1-RON2L complex controls parasitemia. In this experiment, 400 μg of IgG from either control (PBS-Freund's adjuvant–immunized mice) or AMA1-RON2L–immunized mice were passively transferred on days −1, 0, and +1 and challenged on day 0 with 10^5 iRBCs using five mice per group. Error bars indicate mean ± SEM. (*I*) Kaplan–Meier curve of the overall survival of animals in *H*.

AMA1-RON2 Complex-Induced Protection is Largely IgG-Mediated. We next evaluated the contribution of antibody or T cells in conferring protection through passive transfer studies. Total IgG (400 μg) or T cells (2×10^6) from animals immunized with the AMA1-RON2L complex were injected i.v. in naïve mice on days −1, 0, and +1, along with a *Py*YM challenge on day 0. Our data suggest that the complex-dependent protection was largely antibody-mediated, because IgG was able to transfer partial protection, but T cells were not (Fig. 1 *H* and *I* and Fig. S1*C*). Our data do not rule out the possibility of a role for T cells together with antibody in mediating complete protection, however.

The *Pf*AMA1-RON2L Complex Induces Qualitatively Better Growth Inhibitory Antibodies. The surprising ability of the *Py*AMA1-RON2L complex to confer complete protection against a virulent *Py*YM challenge in mice prompted us to evaluate the potential of the AMA1-RON2L complex as a blood-stage vaccine candidate for the human malaria parasite *Pf*. In the absence of an easily accessible in vivo model for human malaria, an in vitro growth inhibition activity (GIA) assay is routinely used to measure the efficacy of antibodies to *Pf* blood-stage antigens (20). We used this GIA assay to compare the efficacy of anti-*Pf*AMA1 and anti–*Pf*AMA1-RON2L antibodies in blocking merozoite invasion.

IgG from rats immunized with *Pf*3D7 allele-AMA1-RON2L complex showed significantly higher inhibition of merozoite invasion against homologous *Pf*3D7 parasites (Fig. 2*A*). This occurred despite comparable levels of antibodies to AMA1 in the animals immunized with AMA1 and those immunized with AMA1-RON2L complex (Fig. 2*B*). Furthermore, antibodies to *Pf*RON2L did not block merozoite invasion at the concentrations tested (Fig. 2*C*), despite the amount of RON2L-specific antibodies was higher in the RON2L-KLH group compared with the AMA1-RON2L group (Fig. S2). Mixing anti-AMA1 and RON2L IgG (AMA1+RON2L-KLH) did not recapitulate the increase in GIA observed with the *Pf*AMA1-RON2L complex (Fig. 2*C*), suggesting that RON2L-specific antibodies do not contribute significantly to GIA at concentrations present in the total IgG.

Inhibitory Antibodies Induced by the AMA1-RON2L Complex Target Mainly AMA1. We next examined the molecular basis of the qualitative difference in the antibodies induced by AMA1 and the AMA1-RON2L complex. We performed competition experiments by adding recombinant *Pf*3D7-AMA1 (rAMA1) to the GIA assays. If the increase in GIA observed with IgG from the *Pf*AMA1-RON2L–immunized rats were related to antibodies targeting new epitopes formed by the complex, then we would have expected that rAMA1 would not completely reverse the GIA of IgG from AMA1-RON2L–immunized rats. Interestingly, a concentration-dependent reversal of GIA was observed when rAMA1 was added to IgG from both *Pf*AMA1- and *Pf*AMA1-RON2L–immunized rats (Fig. 2*D*). This suggests that inhibitory antibodies targeting AMA1 still compose a major part of the GIA of IgG induced by the *Pf*AMA1-RON2L complex. Thus, the qualitative increase in GIA may be related to a difference in the proportion of inhibitory antibodies in the IgG from AMA1- and AMA1-RON2L complex-immunized rats.

This possibility is supported by our observation that IgG from *Pf*AMA1-RON2L complex-immunized animals inhibited RON2L binding to AMA1 significantly higher than IgG induced by *Pf*AMA1 (Fig. 2*E*). Nonetheless, we cannot rule out the contribution of antibodies targeting new epitopes formed by the *Pf*AMA1-RON2L complex, which in the absence of antibodies to AMA1 might not be sufficient to show significant GIA in this in vitro assay.

The *Pf*AMA1-RON2L Complex Induces a Switch in the Proportion of Antibodies to Loops Surrounding the RON2L-Binding Site. The hydrophobic groove in AMA1 is formed by two cysteine-rich domains (21), and binding of RON2L displaces the conserved loop in domain 2 (DII) (18). In addition, domain 1 loops DIb and DIf, which were disordered in the apo structure (Fig. 3*A*),

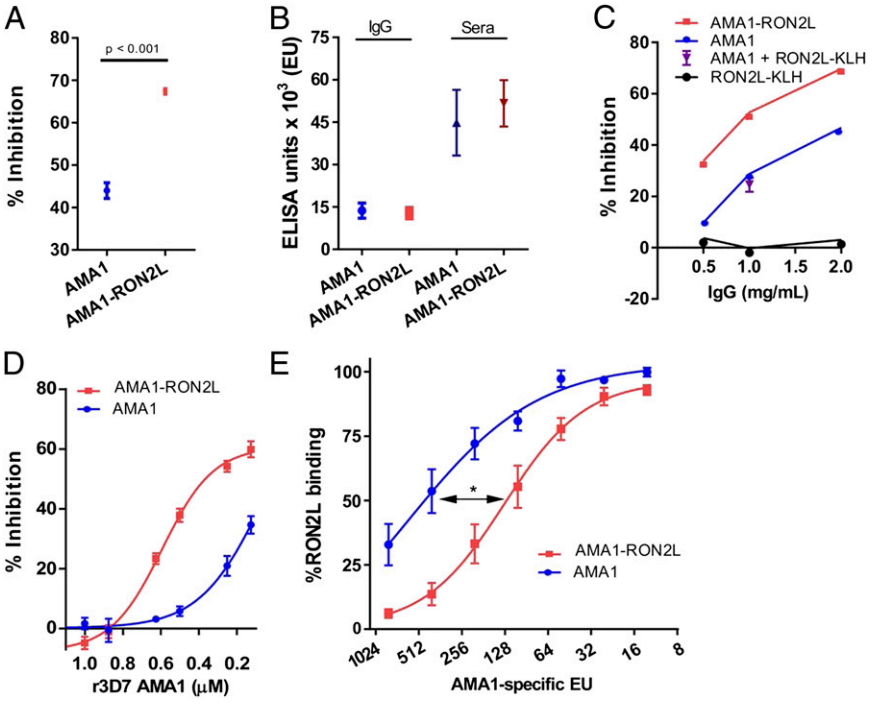

Fig. 2. The *Pf*AMA1-RON2L complex generates better-quality *Pf* invasion-inhibitory antibodies than *Pf*AMA1. (*A*) IgG purified from rats immunized with *Pf*3D7-AMA1-RON2L complex induced greater growth inhibition compared with IgG from *Pf*AMA1-immunized rats ($n = 4$). 2 mg/mL IgG was used in the inhibition assay and results are mean ± SEM of pooled data from two independent experiments. (*B*) *Pf*AMA1 and *Pf*AMA1-RON2L complex induced similar levels of anti-AMA1 antibodies. ELISA units (EU) represent the AMA1-specific antibody titer in purified IgG (2 mg/mL) and serum from four immunized rats used in *A*. Error bars indicate mean ± SEM. (*C*) GIA was performed using increasing concentrations of IgG from the AMA1, RON2L, and AMA1-RON2L groups. Data shown are the mean parasite inhibition from an assay performed in duplicate. The contribution of anti-RON2L antibody toward the increased GIA observed in the AMA1-RON2L group was analyzed by mixing 1 mg/mL each of anti-RON2L IgG and anti-AMA1 IgG (AMA1 + RON2L). Data shown are mean ± SEM for four rats. (*D*) Inhibition of invasion was reversed by the addition of recombinant *Pf*3D7-AMA1 to IgG from *Pf*AMA1 (blue) and *Pf*AMA1-RON2L (red) groups. Data shown are the mean ± SEM parasite inhibition from two independent experiments performed in duplicate. All four data points are plotted. (*E*) Binding of biotinylated RON2L peptide to immobilized *Pf*3D7-AMA1 inhibited by serial dilution of IgG against *Pf*AMA1 (blue) and *Pf*AMA1-RON2L complex (red). The *x*-axis indicates the amount of total AMA1-specific EU present at each of the dilutions. EC_{50} (50% inhibition of RON2L binding) was measured by plotting a nonlinear fit of the individual data points. *$P = 0.018$.

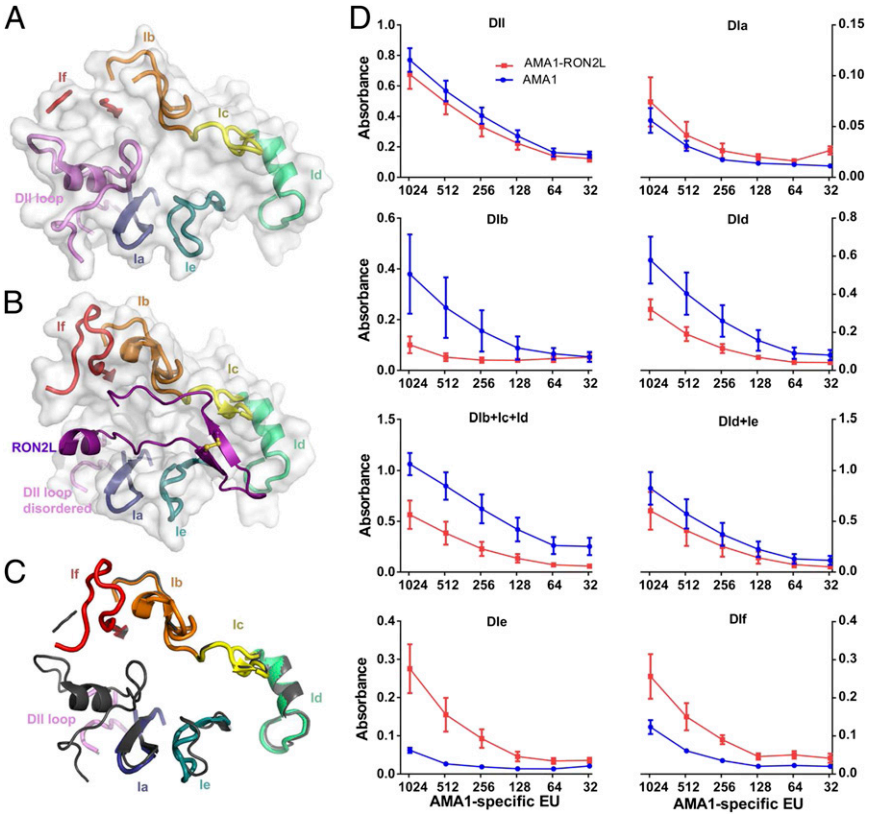

Fig. 3. Proportion of anti-AMA1 and anti–AMA1-RON2L complex IgG to loop regions surrounding the AMA1 hydrophobic groove. (*A*) View of the loops surrounding the hydrophobic groove in the absence of RON2L. (*B*) View of the loops in the RON2L-bound form. (*C*) Overlay of AMA1 loop structures surrounding the hydrophobic groove in the presence (colored) and absence of RON2L (gray). (*D*) Binding of IgG from AMA1 (blue) and AMA1-RON2L complex (red) to biotinylated peptides immobilized on streptavidin plates. The *x*-axis indicates the amount of total AMA1-specific EU present at each of the dilutions. Data are mean ± SEM ($n = 4$). An experiment representative of three independent experiments is shown.

became visible in the complex structure (Fig. 3*B*), along with a conformational change in loop DIe (Fig. 3*C*). Previous studies demonstrated a positive correlation between the amount of antibodies to loop DId and in vitro GIA (10), suggesting that loop regions could be targets of protective immune responses. We hypothesized that some of the conformational changes and/or stabilization of the loops occurring upon RON2 binding might have contributed to the qualitative increase in inhibitory antibodies induced by the complex, and thus we examined the proportion of antibodies against synthetic biotinylated loop peptides by ELISA (Fig. 3*D*).

Surprisingly, whereas the proportion of antibodies against loop DId appeared to be higher in the group immunized with AMA1 alone, levels of antibodies to loops DIe and DIf appeared to be higher in the group immunized with the AMA1-RON2L complex (Fig. 3*D*). Interestingly, the immune response against the DII loop, which undergoes the greatest conformational change, appears to be similar in the two groups (Fig. 3*D*). DId contains some of the highly polymorphic residues, including E197, which has been shown to be a target of strain-specific anti-AMA1 antibodies (22), whereas loops DIe and DIf are less polymorphic (Fig. S3). Our data suggest that a switch in the proportion of antibodies targeting these loops may contribute to the enhanced efficacy of the AMA1-RON2L complex vaccine. This suggestion is supported by a recent study showing that monoclonal antibodies targeting loop DIe potently inhibited parasite invasion (11).

IgG Against the *Pf*3D7-AMA1-RON2L Complex Does Not Block Invasion by the Heterologous *Pf*FVO Clone. As discussed above, the qualitative increase in inhibition mediated by the complex-induced antibodies appears to be related, at least in part, to a switch in the proportion of antibodies targeting loop regions surrounding the RON2-binding site (Fig. 3*D*); however, even these loops are polymorphic, albeit to a lesser extent than such loops as Id (Fig. S3). Thus, if the new inhibitory antibodies induced by the complex target these sites, then the increased efficacy of the complex-induced IgG might be dependent on the sequence of the loops surrounding the AMA1 hydrophobic grove.

We first analyzed the contribution of conserved vs. polymorphic sites by performing antigen-reversal GIA experiments using 3D7 and FVO-allele rAMA1 with 3D7 parasites. If the complex induces antibodies against mainly conserved epitopes, then using saturating amounts of recombinant FVO-allele AMA1 would deplete the GIA activity of complex-induced IgG. However, if the complex induces more growth-inhibitory antibodies targeting variable, albeit less polymorphic residues, then substantially higher GIA compared with AMA1-alone IgG would be expected. Our data show that depleting antibodies to conserved epitopes reversed the GIA of AMA1-alone IgG to baseline levels, but substantially higher GIA was retained in the AMA1-RON2L complex IgG despite the use of comparable amounts of anti-AMA1 antibodies in the two groups (Fig. 4*A*). Consistent with these data, both AMA1- and the AMA1-RON2L complex-induced IgG failed to inhibit FVO parasites at 2 mg/mL (Fig. 4*B*). Instead, inhibition required more antibody (5 mg/mL), perhaps reflecting blocking by common epitopes on AMA1.

Conclusions

In this study, we demonstrate a novel approach toward developing a vaccine against the disease-causing forms of the malaria parasite. The lack of protection in humans immunized with AMA1 has been attributed to insufficient amounts of antibody generated using currently available adjuvants and the polymorphisms between the vaccine type and parasite strains in the field; however, the lack of protection against a controlled, homologous parasite challenge despite the vaccine inducing high anti-AMA1 titers (5) suggests that this might not be the only reason for the failure in human trials.

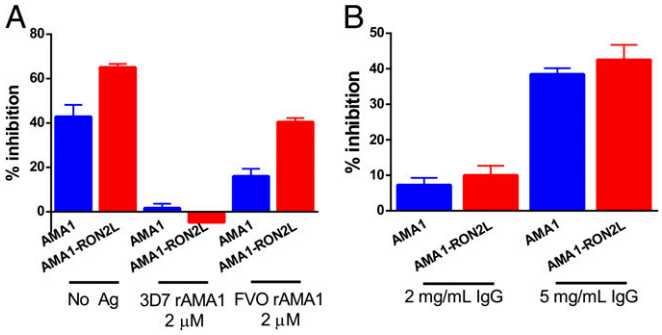

Fig. 4. GIA reversal assay and GIA against a heterologous parasite. (*A*) GIA reversal of 3D7 parasite invasion by homologous 3D7 recombinant AMA1 (2 μM) and heterologous FVO AMA1 (2 μM) when added to IgG (2mg/ mL) from *Pf*AMA1 (blue) and *Pf*AMA1-RON2L (red) groups. Data are mean ± SEM parasite inhibition from two independent experiments performed in duplicate. All four data points are plotted. (*B*) GIA of IgG from *Pf*AMA1 (blue) and *Pf*AMA1-RON2L (red) against heterologous FVO strain parasite. Data are mean ± SEM parasite inhibition performed at 2 mg/mL (four rats each from the AMA1 and AMA1-RON2L groups) and 5 mg/mL (three rats from the AMA1 group and four rats from the AMA1-RON2L group) performed in duplicate.

We provide evidence using *Py* and *Pf*, two independent host–parasite systems, that despite similar AMA1 antibody titers, the AMA1-RON2L complex is more effective in inducing invasion-inhibitory, protective antibodies. Our results suggest that the increased inhibitory activity of IgG induced by the *Pf*AMA1-RON2L complex is related, at least in part, to antibodies that target new AMA1 epitopes surrounding the RON2-binding site. The fact that some of these target sites are less polymorphic bodes well for the development of an effective AMA1-based vaccine. Recent studies suggest that immunization with only four or five AMA1 alleles is sufficient to cover polymorphisms and block multiple parasite strains in vitro (9, 11).

Our results have important implications for developing an effective blood-stage malaria vaccine. For instance, a multiallele AMA1 (to cover polymorphisms) in complex with RON2L should be more effective in protecting against both homologous and heterologous parasites. Furthermore, many of the subunit malaria vaccine candidates under study are present in complexes with one or more binding partners. It is tempting to speculate that our approach of using a protein complex mimicking the functional form of the proteins instead of the individual components may offer clues to the development of the next-generation vaccine candidates for malaria as well as other pathogens.

Methods

Recombinant Protein Production and Peptide Synthesis. ***Escherichia coli* expression.** Synthetic codon optimized *Py*YM AMA1 (residues 59–479; PlasmoDB accession no. PYYM_0916000) with a C-terminal histidine tag was cloned into a pET24a vector. Solubilized inclusion bodies were refolded and affinity-purified essentially as described previously (9). In brief, solubilized protein was purified on a Ni Sepharose 6 FF column (GE Healthcare), followed by separation on a Q Sepharose FF column (GE Healthcare) using 20 mM Tris and a NaCl gradient at pH 8.0. The Ec*Py*AMA1 eluates were pooled and polished on a S75 size-exclusion column (GE Healthcare) with a mobile phase consisting of PBS (pH 7.4). Purified recombinant Ec*Py*AMA1 was characterized by Coomassie blue- stained SDS/PAGE gel electrophoresis, Western blot analysis using a protective, conformational mAb 45B1 (23), reversed-phase HPLC, and analytical size-exclusion column chromatography with online multiangle light-scattering HPLC (Fig. S4), essentially as described previously (24).

***Pichia pastoris* expression.** Recombinant his-tagged *Pf*3D7 and *Pf*FVO AMA1 full-length ectodomain (residues 25–546), as described previously (25), were used in these studies.

Peptide synthesis. All peptides, listed in Fig. S5, were synthesized by LifeTein (South Plainfield, NJ). KLH conjugation to RON2L was also performed by LifeTein.

Parasites and Mouse Infections. *Py*YM parasites were maintained by serial blood passage in BALB/c mice (Charles River Laboratory). For challenge studies after vaccination, the indicated numbers of iRBCs were injected i.v., and parasitemia was measured by counting the number of iRBCs on Giemsa-stained blood smears: % parasitemia = (number of iRBCs*100)/number of total RBCs. All experiments were performed in accordance with National Institutes of Health-approved animal study protocol LMVR-11E.

AMA1-RON2L Complex Preparation, Immunization, and Passive Transfer Studies. The AMA1-RON2L complex was prepared by mixing 10 μg of AMA1 with 30 μg of RON2L in 50 μL of PBS and then incubating the mixture at room temperature for 30 min. The complex was emulsified in 50 μL of Freund's adjuvant. For AMA1 alone or RON2L-KLH alone, 10 μg and 30 μg, respectively, were added to 50 μL of PBS and emulsified in an equal volume of adjuvant. BALB/c mice were immunized s.c. three times (Freund's complete followed by two injections in Freund's incomplete adjuvant) at 3-wk intervals. The control mice received 50 μL of PBS emulsified in an equal volume of adjuvant. The challenge with *Py*YM iRBCs was done at 3 wk after the last immunization. For injecting antigens in separate sites, 10 μg of *Py*AMA1 and 30 μg of *Py*RON2L in 50 μL of PBS were emulsified separately with adjuvant and injected on opposite sides.

For passive transfer studies, IgG from animals immunized with the *Py*AMA1-RON2L complex or control PBS as described above were purified on protein G agarose beads (GE Health Sciences) and dialyzed against RPMI 1640 medium. On days −1, 0, and +1, 400 μg of IgG was injected i.v. into recipient mice. These mice were challenged with 10^5 *Py*YM iRBCs on day 0. T cells from immunized animals were purified using a mouse pan T-cell isolation kit (Miltenyi; 130-095-10). All preparations used contained >80% live cells as measured by counting trypan blue-stained cells. 2×10^6 purified T cells were injected on days −1, 0, and +1, with a challenge with 10^5 *Py*YM iRBCs on day 0. Fig. 1 *A* and *G* shows two independent experiments with mice immunized with AMA1 and/or RON2L separately. Data from two of three independent experiments were performed with the AMA1-RON2L complex are shown in Fig. 1*A* and1G. A third experiment with the AMA1-RON2L complex in Montanide ISA720 adjuvant also demonstrated complete protection. Data from one of three independent immunizations performed with AMA1-RON2L*c*/a (that does not form a complex) are shown in Fig. 1*F*.

For *Pf* studies, four Sprague–Dawley rats (Charles River Laboratory) per group were immunized s.c. with *Pf*3D7 full-length AMA1 (10 μg), RON2L-KLH (10 μg), or AMA1-RON2L complex (10 μg of AMA1 mixed with 30 μg of RON2L) emulsified in Freund's complete adjuvant, followed by two injections in Freund's incomplete adjuvant at 3-wk intervals as described above. IgG from sera of individual rats was purified on a protein G column (GE Health Sciences) and dialyzed against RPMI 1640. Rat immunizations were carried out in accordance with National Institutes of Health-approved animal study protocol LMVR-1.

ELISA. A detailed description of the ELISA procedure is provided elsewhere (26). ELISA plates were coated overnight with 1 μg/mL recombinant AMA1 or 4 μg/mL RON2L peptide. For measuring relative antibodies in immunized mice, a serial dilution of the sera was performed, and the dilution that produced an OD >0.5 (1:8000 for AMA1 and 1:2000 for RON2L) was used to compare the anti-AMA1 and anti-RON2L antibodies between the groups.

Antigen-specific ELISA units for *Pf*AMA1 and *Pf*RON2L were measured by first generating a standard curve using a serially diluted IgG mixture containing either anti-AMA1 (IgG from four rats immunized with AMA1) or RON2L (IgG from four rats immunized with RON2L-KLH). Antibody units of the standards were assigned based on the reciprocal of the dilution giving an OD_{405} of 1, and all samples were tested against the same standard, as described previously (26).

Antibodies to different loop region peptides were measured by first coating individual biotinylated peptides (4 μg/mL) onto streptavidin-coated plates for 2 h at room temperature, followed by the standard ELISA method as described above. To compare the proportion of antibodies in the AMA1 and AMA1-RON2L groups, each IgG sample was adjusted to have the same amount of anti-AMA1 ELISA units.

Competition ELISA was performed as described above with the addition of 0.5 μg/mL biotinylated *Pf*RON2L peptide along with the IgG dilutions (containing the indicated AMA1-EU), to measure the antibodies' ability to inhibit RON2L binding to *Pf*3D7-AMA1. Streptavidin conjugated to alkaline

MICROBIOLOGY

phosphatase (Life Technologies; S-921, 1:2,000 dilution) was used to measure the amount of biotinylated RON2L bound to AMA1.

***Pf* Parasite Culture.** Parasites were maintained in standard in vitro cultures as described previously (27) with modifications as follows. In brief, parasites were grown in RPMI 1640 supplemented with 25 mM Hepes and 50 μg mL^{-1} hypoxanthine (KD Medical), 0.5% Albumax (Invitrogen), and 0.23% sodium bicarbonate (Gibco) using O^+ RBCs (Interstate Blood Bank), and monitored daily by Giemsa-stained blood smears.

GIA. Purified IgG at the desired concentration was dialyzed against RPMI 1640 (KD Medical) and incubated with iRBCs for 40 h. Parasitemia was quantified by biochemical measurement using a *Pf* lactate dehydrogenase assay as described previously (28). GIA reversal was performed by mixing the desired concentration of recombinant proteins with 2 mg/mL pooled IgG from four rats in each group and then adding this mixture to the GIA wells. All assays were performed in duplicate.

Homology Modeling of the *Py*AMA1-*Py*RON2_D3 Complex. The structural model for *Py*AMA1 (Asn53–Glu383; XP_729363.1) was generated using Modeler 9v8 through the Chimera interface (29, 30), based on a hybrid model of *Pf*AMA1 [Protein Data Bank (PDB) ID code 3ZWZ] and *Pv*AMA1 (PDB ID code 1Z40), with which it shares 52% and 56% identity, respectively. The region of the DII loop (Lys296–Ser332) disordered in the *Pf*AMA1 costructure with *Pf*RON2_D3 and in the apo structure of *Pv*AMA1 was removed owing to uncertainty in its position while in complex with *Py*RON2_D3. The final model of *Py*AMA1 was chosen based on the low value of the normalized discrete optimized protein energy value (zDOPE).

The 30 core residues *Py*RON2_D3 (His2068–Val2097; XP_727536.1) were modeled based on *Pf*RON2_D3 from the published costructure with *Pf*AMA1 (18), and were initially docked into the *Py*AMA1 groove using ProtInfoPPC (31). The *Py*AMA1-*Py*RON2_D3 model was refined using Rosetta FlexPepDock (32), with the complex with the lowest Rosetta energy score chosen and validated by visual inspection, PISA (33), ProQ (34), ERRAT (35), and MolProbity (36).

Statistical Analysis. Differences in GIA responses in IgG from the *Pf*AMA1 and *Pf*AMA1-RON2L groups were measured using the nonparametric Mann–Whitney test. Inhibition of RON2L binding to AMA1 was measured by plotting a nonlinear regression curve fit of the individual data points and comparing the EC_{50} of the two curve fits.

ACKNOWLEDGMENTS. We thank Dr. Susan Pierce for a critical reading of the manuscript, Dr. Patrick Duffy for valuable suggestions, and Dr. Nicholas MacDonald, Dr. Harold Obiakor, Raul Herrera, and Karine Reiter from the Process Development Unit for their excellent technical assistance. These studies were supported by the Intramural Research Program of the Division of Intramural Research, National Institute of Allergy and Infectious Diseases, National Institutes of Health and by the Canadian Institutes for Health Research [Research Grant MOP82915 (to M.J.B.)].

1. Murray CJ, et al. (2012) Global malaria mortality between 1980 and 2010: A systematic analysis. *Lancet* 379(9814):413–431.
2. Olotu A, et al. (2013) Four-year efficacy of RTS,S/AS01E and its interaction with malaria exposure. *N Engl J Med* 368(12):1111–1120.
3. Stowers AW, et al. (2002) Vaccination of monkeys with recombinant *Plasmodium falciparum* apical membrane antigen 1 confers protection against blood-stage malaria. *Infect Immun* 70(12):6961–6967.
4. Dutta S, et al. (2009) High antibody titer against apical membrane antigen-1 is required to protect against malaria in the Aotus model. *PLoS ONE* 4(12):e8138.
5. Spring MD, et al. (2009) Phase 1/2a study of the malaria vaccine candidate apical membrane antigen-1 (AMA-1) administered in adjuvant system AS01B or AS02A. *PLoS ONE* 4(4):e5254.
6. Ouattara A, et al. (2010) Lack of allele-specific efficacy of a bivalent AMA1 malaria vaccine. *Malar J* 9:175.
7. Thera MA, et al. (2011) A field trial to assess a blood-stage malaria vaccine. *N Engl J Med* 365(11):1004–1013.
8. Drew DR, et al. (2012) Defining the antigenic diversity of *Plasmodium falciparum* apical membrane antigen 1 and the requirements for a multi-allele vaccine against malaria. *PLoS ONE* 7(12):e51023.
9. Miura K, et al. (2013) Overcoming allelic specificity by immunization with five allelic forms of *Plasmodium falciparum* apical membrane antigen 1. *Infect Immun* 81(5): 1491–1501.
10. Ouattara A, et al. (2013) Molecular basis of allele-specific efficacy of a blood-stage malaria vaccine: Vaccine development implications. *J Infect Dis* 207(3):511–519.
11. Dutta S, et al. (2013) Overcoming antigenic diversity by enhancing the immunogenicity of conserved epitopes on the malaria vaccine candidate apical membrane antigen-1. *PLoS Pathog* 9(12):e1003840.
12. Remarque EJ, Faber BW, Kocken CH, Thomas AW (2008) A diversity-covering approach to immunization with *Plasmodium falciparum* apical membrane antigen 1 induces broader allelic recognition and growth inhibition responses in rabbits. *Infect Immun* 76(6):2660–2670.
13. Lamarque M, et al. (2011) The RON2–AMA1 interaction is a critical step in moving junction-dependent invasion by apicomplexan parasites. *PLoS Pathog* 7(2):e1001276.
14. Tyler JS, Boothroyd JC (2011) The C-terminus of *Toxoplasma* RON2 provides the crucial link between AMA1 and the host-associated invasion complex. *PLoS Pathog* 7(2): e1001282.
15. Srinivasan P, et al. (2011) Binding of *Plasmodium* merozoite proteins RON2 and AMA1 triggers commitment to invasion. *Proc Natl Acad Sci USA* 108(32):13275–13280.
16. Srinivasan P, et al. (2013) Disrupting malaria parasite AMA1–RON2 interaction with a small molecule prevents erythrocyte invasion. *Nat Commun* 4:2261.
17. Richard D, et al. (2010) Interaction between *Plasmodium falciparum* apical membrane antigen 1 and the rhoptry neck protein complex defines a key step in the erythrocyte invasion process of malaria parasites. *J Biol Chem* 285(19):14815–14822.
18. Vulliez-Le Normand B, et al. (2012) Structural and functional insights into the malaria parasite moving junction complex. *PLoS Pathog* 8(6):e1002755.
19. Tonkin ML, et al. (2011) Host cell invasion by apicomplexan parasites: Insights from the co-structure of AMA1 with a RON2 peptide. *Science* 333(6041):463–467.
20. Kennedy MC, et al. (2002) In vitro studies with recombinant *Plasmodium falciparum* apical membrane antigen 1 (AMA1): Production and activity of an AMA1 vaccine and generation of a multiallelic response. *Infect Immun* 70(12):6948–6960.
21. Pizarro JC, et al. (2005) Crystal structure of the malaria vaccine candidate apical membrane antigen 1. *Science* 308(5720):408–411.
22. Coley AM, et al. (2006) The most polymorphic residue on *Plasmodium falciparum* apical membrane antigen 1 determines binding of an invasion-inhibitory antibody. *Infect Immun* 74(5):2628–2636.
23. Narum DL, Ogun SA, Thomas AW, Holder AA (2000) Immunization with parasite-derived apical membrane antigen 1 or passive immunization with a specific monoclonal antibody protects BALB/c mice against lethal *Plasmodium yoelii yoelii* YM blood-stage infection. *Infect Immun* 68(5):2899–2906.
24. Plassmeyer ML, et al. (2009) Structure of the *Plasmodium falciparum* circumsporozoite protein, a leading malaria vaccine candidate. *J Biol Chem* 284(39):26951–26963.
25. Ellis RD, et al. (2012) Phase 1 study in malaria naïve adults of BSAM2/Alhydrogel®+ CPG 7909, a blood-stage vaccine against *P. falciparum* malaria. *PLoS ONE* 7(10): e46094.
26. Miura K, et al. (2008) Comparison of biological activity of human anti-apical membrane antigen-1 antibodies induced by natural infection and vaccination. *J Immunol* 181(12):8776–8783.
27. Trager W, Jensen JB (1976) Human malaria parasites in continuous culture. *Science* 193(4254):673–675.
28. Malkin EM, et al. (2005) Phase 1 clinical trial of apical membrane antigen 1: An asexual blood-stage vaccine for *Plasmodium falciparum* malaria. *Infect Immun* 73(6): 3677–3685.
29. Pettersen EF, et al. (2004) UCSF Chimera—a visualization system for exploratory research and analysis. *J Comput Chem* 25(13):1605–1612.
30. Eswar N, et al. (2006) Comparative protein structure modeling using Modeller. *Curr Protoc Bioinformatics* Chapter 5:Unit 5.
31. Kittichotirat W, Guerquin M, Bumgarner RE, Samudrala R (2009) Protinfo PPC: A web server for atomic level prediction of protein complexes. *Nucleic Acids Res* 37(Web Server issue):W519–W525.
32. London N, Raveh B, Cohen E, Fathi G, Schueler-Furman O (2011) Rosetta FlexPepDock web server: High-resolution modeling of peptide–protein interactions. *Nucleic Acids Res* 39(Web Server issue):W249–W253.
33. Krissinel E, Henrick K (2007) Inference of macromolecular assemblies from crystalline state. *J Mol Biol* 372(3):774–797.
34. Wallner B, Elofsson A (2003) Can correct protein models be identified? *Protein Sci* 12(5):1073–1086.
35. Colovos C, Yeates TO (1993) Verification of protein structures: Patterns of nonbonded atomic interactions. *Protein Sci* 2(9):1511–1519.
36. Chen VB, et al. (2010) MolProbity: All-atom structure validation for macromolecular crystallography. *Acta Crystallogr D Biol Crystallogr* 66(Pt 1):12–21.